Available online at www.sciencedirect.com

ScienceDirect

Procedia Structural Integrity 43 (2023) 160–165

Structural Integrity Procedia

www.elsevier.com/locate/procedia

10th International Conference on Materials Structure and Micromechanics of Fracture

Effects of annealing temperature on microstructure and mechanical properties of cold sprayed AA7075

Jakub Judas[a*], Josef Zapletal[a], Lukáš Řehořek[a], Vít Jan[a]

[a] *Brno University of Technology, Faculty of Mechanical Engineering, Brno, Czech Republic*

Abstract

This paper examines the softening behaviour of cold sprayed 7075 aluminum alloy after isothermal annealing. The as-received powder was deposited by a high-pressure cold spray device using heated nitrogen as propellant gas. To investigate the effects of post-deposition heat treatment, the excised samples were isochronally annealed in the temperature range of 200 to 400 °C. The feedstock powder and the free-standing coatings were initially characterized through various electron microscopy techniques (SEM, EDS, EBSD) and relevant microstructural features were determined. Mechanical properties of the as-sprayed and heat-treated samples were evaluated by quasi-static tensile and microhardness testing. It has been shown that extensive plastic deformation during cold spraying resulted in a dense coating with relatively low internal porosity. Specimens in an as-deposited state possessed a high level of strain hardening and exhibited a brittle rupture associated with intersplat cracking. When subjected to heat treatment, the cold spray deposits showed a general trend of microhardness reduction and progressive sintering of the microstructure with increasing annealing temperature. Furthermore, post-mortem observation revealed a gradual transition in fracture mechanism, manifested by improving material ductility and the occurrence of typical dimple morphology. The aspects responsible for the softening of the cold sprayed 7075 alloys are discussed further.

Keywords: Cold Spray; 7075 aluminum alloy; isothermal annealing; tensile testing; electron microscopy

1. Introduction

Cold gas dynamic spraying (or simply Cold spray, CS) is a solid-state coating technology, in which feedstock powder particles (5-100 μm) are accelerated onto the substrate by an expanding gas stream at temperatures below the melting point of the material. The formation of CS coatings predominantly relies on extensive plastic deformation of micron-sized particles, resulting in the formation of metallurgical bonds during impact through the adiabatic shear instability mechanism. In contrast to conventional thermal spraying techniques, detrimental effects on coating

* Corresponding author. Tel.: +420-702-498-240
*E-mail address:*jakub.judas@email.cz

10.1016/j.prostr.2022.12.252

properties such as oxidation, phase transformation, non-equilibrium microstructure, or crack formation during rapid solidification are reduced (Marzbanrad et al. (2021)). These process characteristics make CS especially suitable for oxidation and thermal sensitive materials (Al, Ti, and Mg alloys).

In cold spraying, the criteria for successful bonding are met only when the powder particles exceed a certain critical impact velocity (generally 300-800 m/s), which is a complex function of process parameters, nozzle shape, and coating-substrate thermomechanical behaviour. The superposition of large strains induced during CS along with the peening and hammering effect of incoming particles subsequently leads to the fabrication of dense coatings with promising mechanical, electrical, and wear properties (Gärtner et al. (2006)). Significant plastic deformation and associated dislocation substructure contribute to a strong work hardening effect during CS deposition (Yang et al. (2018)). CS deposits, however, exhibit very low ductility as a consequence of heavily worked microstructure and some degree of porosity (Huang et al. (2017)). To overcome this shortcoming, post-deposition heat treatment is frequently employed to improve the plasticity and structural integrity of CS coatings (Rokni et al. (2017)).

The 7xxx series Al alloys are widely used in numerous industries, e.g., aviation, automotive, marine, defence, and robotics. Among them, the 7075 precipitation-hardenable alloy is probably the most popular due to its high strength-to-weight ratio, fatigue resistance, and excellent machinability (Marzbanrad et al. (2021)). Considering that CS is a potential candidate for repairing damaged parts in the aerospace industry, several attempts have been made to produce aluminum alloy 7075 via CS technology. Rokni et al. (2015) studied the effects of non-isothermal annealing on the softening behaviour of cold-sprayed 7075 and described substructure changes during the thermal cycle. Xiong et al. (2015) reported opposing effects of substrate preheating on bond strength variations with the coating thickness. More recently, Sabard et al. (2020) investigated the influences of powder heat treatment on coating densification and revealed an inverse relationship between deposition efficiency and resulting cohesive strength.

In most of the previously mentioned research papers, helium was used as a propellant gas because its lower molecular weight and higher specific heat ratio generally lead to better coating properties (Gärtner et al. (2006)). However, for industrial applications, nitrogen is usually the first choice owing to its lower cost (Bobzin et al. (2021)). The aim of the present work is to examine the annealing behaviour of the CS 7075 alloy using nitrogen as a process gas. Tensile tests, microhardness measurement and microscopic observations are utilized to determine the effects of the applied heat treatment. The results are then analyzed and discussed with the available literature.

2. Materials and methods

2.1. Feedstock powder and cold spray processing

Gas-atomized 7075 Al powder (Nanografi, Turkey) with the following chemical composition (wt%): 5.57 Zn, 1.99 Mg, 1.66 Cu, 0.26 Si, 0.21 Cr, and Al balance was deposited on rectangular (50x40 mm) 6082-T6 substrates, which were grit blasted and preheated prior to coating deposition. The spherical morphology of the powder with an overall distribution range of 15-48 μm is shown in Fig. 1. In this study, a commercial high-pressure 5/11 cold spray system (Impact Innovations, GmbH, Germany) was employed with nitrogen as the process gas. The pressure and temperature of nitrogen were maintained at 4 MPa and 550 °C, respectively, at the outlet of the heater. The fabrication took place using a nozzle standoff distance of 30 mm, track spacing of 1 mm, deposition angle of 90°, and relatively high scanning speed (300 mm/s). The target coating thickness was set at 3 mm (approximately 20 gun passes).

2.2. Heat treatment and mechanical properties

After spraying, the 7075 aluminum deposits were removed from the substrates by cutting with wire electrodes and subsequently subjected to a post-deposition heat treatment consisting of isothermal annealing at temperatures of 200, 300, and 400 °C for the same exposure time of 3 hours. All heat treatments were carried out in an open-air furnace PP49/65 (LAC, Czech Republic), and then the samples were left inside the furnace to cool to room temperature.

Uniaxial tensile tests on as-sprayed and heat-treated coatings were performed at an ambient temperature under displacement rate control of 0.5 mm/min using a universal testing device (Zwick/Roell Z250, Germany) equipped with a high-accuracy multiXtens extensometer, and the corresponding engineering stress-strain response was determined. The tensile samples were machined out of the coatings so that the tensile axis was perpendicular to the

spraying direction (depicted in Fig. 2). A total of 12 specimens (three for each condition) were stretched according to the standard EN ISO 6892-1 and then the microstructure obtained from their clamping part was examined.

Microhardness measurements were also performed on the CS 7075 coatings in both the as-deposited and thermally treated conditions using a Vicker´s Qness Q10A microhardness tester (QATM, GmbH, Germany) with an indenter load of 100 g and a dwell time of 15 s. Twelve points across the entire coating thickness were tested in both the longitudinal plane (scanning, XY) and the transverse plane (loading, YZ) for each sample to account for possible variations in micromechanical properties in these two directions. The measurements for the points with extreme values (maximum and minimum values) were discarded, and the mean hardness and its standard deviation were reported.

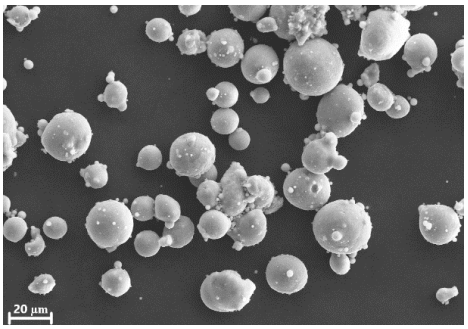

Fig. 1. Morphology of 7075 aluminum powder.

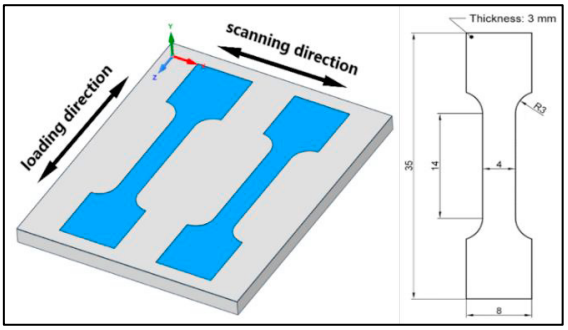

Fig. 2. The sketch map of tensile specimen orientation and its geometry.

2.3 Microstructure and fractographic characterization

Cross-sections of as-sprayed and heat-treated CS deposits were prepared by a conventional metallographic technique, i.e., mechanical grinding with SiC papers up to 4000 grit size, followed by polishing with 3 µm and 1 µm diamond paste. The last step was conducted through mechano-chemical polishing with a non-drying Struers OP-S suspension. The porosity of all coatings was evaluated by image analysis using ImageJ software in three parallel planes (average distance of 1 mm) to ensure repeatability of results. Electron backscattered diffraction (EBSD, Oxford Instruments) was employed in the research to study the grain size distribution and misorientation angle. The fracture surfaces of broken specimens were observed with a scanning electron microscope (ULTRA PLUS, Carl Zeiss, Germany) to explore the failure mechanism. Energy-dispersive X-ray spectroscopy (Aztec, Oxford Instruments) was used for the chemical identification of present phases.

3. Results and discussions

3.1. Microstructural analysis

SEM micrographs obtained from the central part of the CS 7075 coating and corresponding EBSD mapping supplemented by band contrast are depicted in Fig. 3 and Fig. 4, respectively. For the sake of brevity, only two opposing conditions (as-built and annealed at 400 °C/3h) were evaluated with cross-sections oriented perpendicular to the scanning direction. The BSE images in Fig. 3 show extensive segregation of dissolved elements in the matrix as a result of rapid solidification (cooling rate between 10^4 and 10^7 K/s) accompanied by a solute rejection (Jones (1984)). This characteristic feature of the as-received powder is retained in the microstructure, although the material has undergone a significant thermomechanical process during the CS deposition. EDS investigation revealed a strongly supersaturated solid solution in the form of bright areas containing, in particular, high concentrations of Zn, Cu and Mg atoms. Subsequent annealing leads to the progressive disintegration of this network and to the growth of precipitates enriched in the main alloying elements at the grain boundaries.

From the inspection of Fig. 4a, the coating microstructure in the as-sprayed state consists of two dissimilar regions, distinguished by their heterogeneous grain structure. The first one is the particle interior which is characterized by coarser grains (1-10 µm in size) with a high density of low-angle grain boundaries (LAGBs, $\theta < 10°$). These are formed by dislocation walls and tangles created by the shot-peening effect of the powder particles during impact (Rokni et. al (2015)). The second region is the particle interface, which is typically smaller in grain size (0.2-1 µm)

and has a somewhat lower incidence of LAGBs. The occurrence of this UFG structure at particle-particle boundaries is attributed to the dynamic recrystallization phenomenon which is caused by the superposition of severe plastic deformation and high temperature during the CS procedure (Kim et al. (2008)). The individual interfaces between the deposited particles are clearly visible in the band contrast images (enclosed in the lower right corner) due to the heavily stressed microstructure associated with the formation of lattice defects as well as the grain deformation.

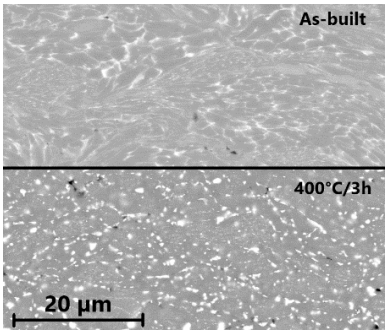

Fig. 3. SEM images of the CS 7075 deposit.

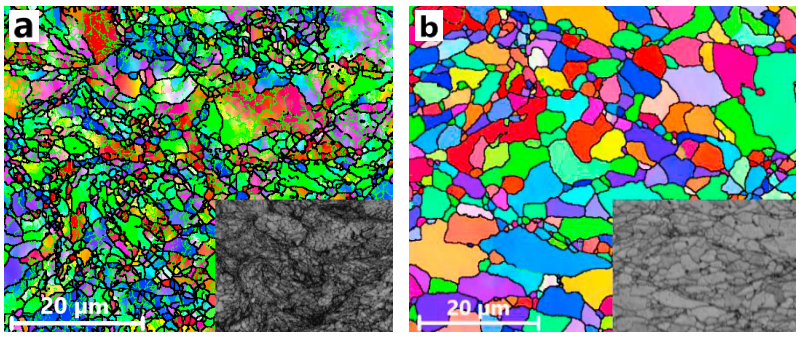

Fig. 4. EBSD maps with the corresponding band contrast: a) as-built; b) annealed at 400°C/3h.

EBSD scans were performed on the heat-treated samples to determine the recovery/recrystallization ability of the CS 7075 alloy. From the examination of Fig. 4b, it is evident that the microstructure in the case of high temperature annealing at 400 °C exhibits a much more uniform grain size distribution throughout the deposit. The signal quality at the respective band contrast figure has improved remarkably compared to the initial state, indicating the annihilation of crystal defects, and representing the polygonization of the microstructure. The result of the misorientation angle distribution shows a sharp increase in the fraction of high-angle grain boundaries (HAGBs, $\theta \geq 10$) during the tempering period. The proportion of calculated HAGBs is 52.1 %, while it is only 26.5 % in the as-deposited state. The transformation of LAGBs into HAGBs is realized by grain rotation and dislocation rearrangement, leading to the restoration of the former undeformed structure (Yang et al. (2018)). The secondary recrystallization process has obviously increased the average grain size (from about 1.2 µm to 2.4 µm) due to the relatively long annealing time. However, this value is surprisingly still almost identical to the grain size of the 7075 powder particles sprayed in this research. This finding indicates superior thermal grain stability, which can be explained by a pronounced precipitation of secondary phases (see Fig. 3), which inhibit grain boundary migration by their pinning effect (Liang et al. (2020)).

3.2. Mechanical properties and porosity measurement

Tensile tests and microhardness measurements were carried out to establish the softening behaviour of the CS 7075 alloy after annealing treatment (Table 1). The as-built coating sample is characterized by a brittle response during static straining (negligible elongation to failure) which has been well documented for deposits upon the CS process (Huang et al. (2015)). This can easily be explained by the numerous defects present in the microstructure and the strong resistance to plastic deformation owing to grain refinement as well as the high level of dislocation hardening (see LAGBs in Fig. 4a). Annealing at a lower temperature of 200 °C resulted in only a slight alteration of the coating microhardness, which could not fundamentally change the corresponding stress-strain curve. Zhao et al. (2004) studied the properties of 7075 ECAP-treated billets with UFG structure (similar to CS) and found that alloy softening started at temperatures above 150 °C, which was associated with the onset of dislocation polygonization and recovery.

A further increase in temperature up to 300 °C leads to a sharp drop in the material microhardness by about 20 % as a consequence of the recrystallization phenomenon and changes in the precipitation substructure. Processing at such an elevated temperature provided sufficient energy to the microstructure to promote complete recrystallization of the CS coating (Souza et al. (2019)). Since AA7075 is a precipitation-hardenable alloy and the powder used is at least partially supersaturated (shown in Fig. 3), it is also necessary to consider the deleterious effects of over-ageing during thermal exposure. The loss of coherency strains and the coarsening of precipitates is therefore another possible mechanism contributing to the softening of the studied CS alloy (Marlaud et al. (2010)). Heating the coating up to 400 °C activates rapid recrystallization due to the extensive plastic deformations caused by the previous shot peening

stresses. The reduction in deposit microhardness is already rather unimpressive compared to annealing at 300 °C owing to the limited grain growth (introduced in Fig. 4b) and the minor changes in precipitate morphology and density (Zhao et al. (2004)). The weakening of the strengthening mechanisms in cooperation with the sintering of intersplat defects significantly improves yielding ability and the resulting ductility of the CS 7075 coating.

Table 1. Mechanical properties and porosity evaluation of the CS 7075 alloy in the as-built and annealed state.

Coating condition	Yield strength [MPa]	Ultimate strength [MPa]	Elongation [%]	Hardness HV0.1 XY / YZ	Porosity [%] XY
As-built	-	245 ± 31	< 0.1	142 ± 6 / 142 ± 9	0.6 ± 0.2
200 °C/3h	-	247 ± 2	< 0.1	129 ± 5 / 128 ± 7	0.4 ± 0.2
300 °C/3h	238 ± 6	246 ± 3	0.3 ± 0.1	100 ± 3 / 102 ± 2	0.4 ± 0.2
400 °C/3h	169 ± 2	225 ± 5	2.9 ± 0.1	91 ± 3 / 92 ± 3	0.3 ± 0.2

3.3. Fracture morphologies of CS coatings

To obtain detailed information on the micromechanism of deformation behaviour, the fracture surfaces of as-sprayed and heat-treated tensile samples were analyzed by SEM in a top view. The fracture morphology of specimens strained after annealing at 200 °C is very similar to the state after deposition and is therefore omitted in the report. The SEM micrographs of broken specimens are illustrated in Fig. 5, which revealed two distinct regions. The first one is connected with undesirable intersplat cracking, which results in a brittle response during preceding tensile loading. Interparticle rupture is a typical phenomenon for CS coatings and leads to rapid propagation of intercrystalline cracks, which could explain the insufficient ductility of the CS 7075 alloy (Huang et al. (2015)). The ductile fracture areas and the characteristic dimple patterns are the second features observed on the broken surface (marked with arrows in Fig. 5a). This morphology is manifested by the micro-void coalescence and its negligible occurrence on the fracture surface indicates the primary role of the interlocking mechanism during the deposition process (Rokni et al. (2017)).

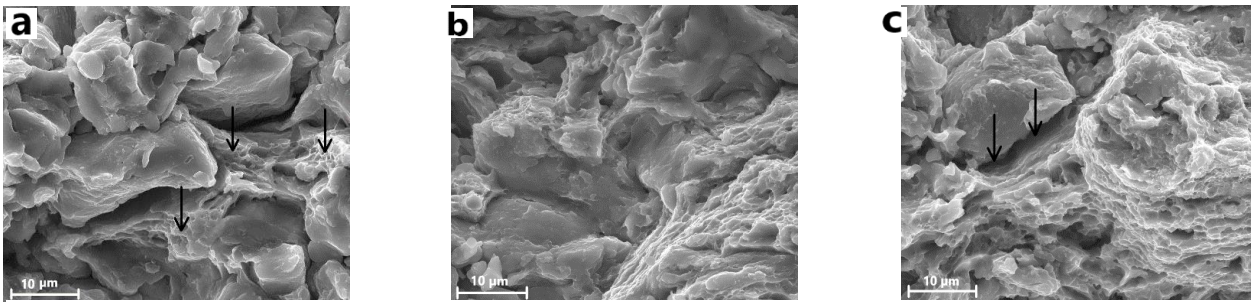

Figure 5. Fracture surfaces of CS 7075 coatings: a) as-sprayed condition; b) annealed at 300 °C/3h; c) annealed at 400 °C/3h.

A low-temperature heat treatment (T < 250°C) is generally not able to support a significant change in fracture behaviour of the CS 7075 alloy due to only slight variations in the mechanical properties of the coating. On the contrary, increasing the annealing temperature up to 300 °C leads to a transition of the fracture mechanism from brittle cracking to ductile failure (Fig. 5b). This is also reflected in the smoother fracture surface, which makes it more difficult to differentiate individual former spray splats. Higher temperatures trigger diffusion-driven processes resulting in continuous recrystallization of the material and reducing the number of interparticle defects as well. Raising the annealing temperature to the highest level of 400 °C induces a substantial increase in the proportion of plastic deformation, which seems to be dominant in the topography. Numerous particles at the bottom of the dimples (0,5-1 µm in size) can be observed at higher magnification as the origin of ductile failure. EDS analysis exposed angular precipitates enriched in Mg and Cu, identified as Al_2CuMg phases (Woznicki et al. (2021)). Although the annealing cycle causes a gradual healing of the coating microstructure, some defects are still found on the broken surface (arrows in Fig. 5c). This makes the specimen fail in the initial stage of plastic deformation and the tensile strength and elongation are lower compared to the bulk material.

4. Conclusions

In this study, CS 7075 aluminum alloy was fabricated to investigate the changes in microstructure and mechanical properties after subsequent isothermal annealing. The main conclusions can be drawn as follows:

- The microstructure of CS 7075 coating consists of two distinct regions, which differ in grain size distribution and show dissimilar strengthening mechanisms, i.e., LAGBs and HAGBs ratio.
- The mechanical properties in the as-built condition are characterized by brittle response during the static straining as a consequence of intersplat defects as well as strong resistance to plastic deformation.
- Post-deposition heat treatment triggers the recovery/recrystallization of the microstructure, leading to a progressive decrease in microhardness and porosity and to the restoration of the coating ductility.
- Examination of the fracture surface revealed a gradual transition in fracture behaviour, associated with a significant amount of low-energy ductile failure at the higher annealing temperature.

Acknowledgements

This work was supported by BUT project no. FSI-S-20-6484. The authors would also like to thank Ing. Igor Moravčík, PhD for performing the EBSD analysis and assisting in the interpretation of the results.

References

Marzbanrad, B., Razmpoosh, M.H., Toyserkani, E., Jahed, H., 2021. Role of heat balance on the microstructure evolution of cold spray coated AZ31B with AA7075. Journal of Magnesium and Alloys 9, 1458-1469.

Gärtner, F., Stoltenhoff, T., Voyer, J., Kreye, H., Riekehr, S., Kocak, M., 2006. Mechanical properties of cold-sprayed and thermally sprayed copper coatings. Surface and Coatings Technology 200, 6770-6782.

Yang, K., Li, W., Yang, X., Xu, Y., 2018. Anisotropic response of cold sprayed copper deposits. Surface and Coatings Technology 335, 219-227.

Huang, R., Sone, M., Ma., W., Fukanuma, H., 2015. The effects of heat treatment on the mechanical properties of cold-sprayed coatings. Surface and Coatings Technology 261, 278-288.

Rokni, M.R., Widener, C.A., Ozdemir, O.C., Crawford, G.A., 2017. Microstructure and mechanical properties of cold sprayed 6061 Al in As-sprayed and heat-treated condition. Surface and Coatings Technology 309, 641-650.

Rokni, M.R., Widener, C.A., Champagne, V.K., Crawford, G.A., 2015. An investigation into microstructure and mechanical properties of cold sprayed 7075 Al deposition. Materials Science & Engineering A 276, 305.315.

Xiong, Y., Zhuang, W., Zhang, M., 2015. Effect of the thickness of cold sprayed aluminium alloy coating on the adhesive bond strength with an aluminium alloy substrate. Surface and Coatings Technology 270, 259-265.

Sabard, A., McNutt, P., Begg, H., Hussain, T., 2020. Cold spray deposition of solution heat treated, artificially aged and naturally aged Al 7075 powder. Surface and Coatings Technology 385, 125367.

Bobzin, K., Wiethegger, W., Hebing, J., Gerdt, L., 2021. Softening Behavior of Cold-Sprayed Aluminum-Based Coatings AA1200 and AA7075 During Annealing. J Therm Spray Tech 30, 358-370.

Jones, H., 1984. Microstructure of Rapidly Solidified Materials. Materials Science & Engineering 65, 145-146.

Kim, K., Watanabe, M., Kawakita, J., Kuroda, S., 2008. Grain refinement in a single titanium powder particle impacted at high velocity. Scripta Materialia 59, 768-771.

Liang, M., Chen, L., Zhao, G., Guo, Y., 2020. Effects of solution treatment on the microstructure and mechanical properties of naturally aged EN AW 2024 Al alloy sheet. Journal of Alloys and Compounds 824, 153943.

Zhao, Y.H., Liao, X.Z., Jin, Z., Valiev, R.Z., Zhu, Y.T., 2004. Microstructures and mechanical properties of ultrafine grained 7075 Al alloy processed by ECAP and their evolutions during annealing. Acta Materialia 52, 4589–4599.

Souza, S.H., Padilha, A.F., Kliauga, A.M., 2019. Softening Behavior During Annealing of Overaged and Cold-rolled Aluminum Alloy 7075. Materials Research 22, 20180666.

Marlaud, T., Deschamps, A., Bley, F., Lefebvre, W., Baroux, B., 2010. Evolution of precipitate microstructures during the retrogression and re-ageing heat treatment of an Al–Zn–Mg–Cu alloy. Acta Materialia 58, 4814-4826.

Woznicki, A., Madej, B.L., Wloch, G., Grzyb, J., Madura, J., Lesniak, D., 2021. Homogenization of 7075 and 7049 Aluminium Alloys Intended for Extrusion Welding. Metals 11, 338.